Journal of
Computational and Theoretical Nanoscience
Vol. 6, 1–9, 2009

Minimal Molecular Models for the Study of Nanostructures

Juan S. Gómez-Jeria

Universidad de Chile, Facultad de Ciencias, P.O. Box 653 Santiago 21, Chile, and Programa de Doctorado en Fisicoquímica Molecular, Universidad Andrés Bello, Facultad de Ecología y Recursos Naturales, República 275, Santiago, Chile

The existence of a minimal molecular model to represent some electronic properties of nanostructures is analyzed for several kinds of nanotubes and graphene surfaces by using the Extended Hückel Theory. It is shown that the use of only the invariance of the electronic chemical potential upon addition of basic units, used to define the minimal molecular model, is not entirely correct. We must add at least the study of the energies and the nature and location of the frontier molecular orbitals. All the results presented here indicate that Extended Hückel Theory is still a valuable tool for the study of the electronic structure of molecular systems possessing great numbers of π electrons.

Keywords: Minimal Molecular Models, Electronic Chemical Potential, Extended Hückel Method, Nanotubes, Graphenes.

RESEARCH ARTICLE

1. INTRODUCTION

Molecular Electronics is a relatively recent scientific discipline that seeks to use individual molecules to perform functions identical or analogous to those of transistors, diodes, conductors and other key components of today's microcircuits. This area of research is now approaching maturity, and the field thus needs scientists having a good understanding of the properties (electrical, chemical and process-related) of organic electronic materials.

Molecular structure and properties are predicted on the basis of theoretical calculations. Such calculations are expected to play a major role in the evolution of molecular electronics. For small and medium-sized molecular systems, first principles quantum chemical calculations can be carried out on a daily basis without any problem. Nevertheless, the systematic calculation of the electronic structure of most macro-nanostructures with *ab initio* or Density Functional methods is not possible yet due to the high computational demands of these kinds of calculations. From the conceptual point of view, a combination of two approaches is possible to deal with this problem.

The first consists in using a lower level of the theory (i.e., a semiempirical method) to get the wavefunction and the associated eigenvalues.

The second is to find a method to obtain a "minimal molecular model," in such a way that we can reasonably assert that the main features of its electronic structure can be extrapolated to bigger ones.

In this paper I will present and discuss previous and new results obtained with the combination of these two approaches.

2. METHODS AND CALCULATIONS

2.1. The Choice of the Method for Calculating the Wavefunction

In 1963, Hoffmann developed a semiempirical quantum mechanical method known as the Extended Hückel Theory[1] (EHT). EHT is the simplest and most primitive of all all-valence-electron methodologies. EHT models all the valence orbitals based on the orbital overlaps and experimental electron affinities and ionization potentials. The diagonal elements of the Hamiltonian are taken as the negative of the normal first ionization energy of the atom corrected by spectroscopic terms to deal with the situation where the normal ionization is not removing the electron from the orbital in question. The off-diagonal matrix elements of the Hamiltonian are calculated according to the modified Wolfsberg-Helmholz formula.[2] The use of experimental ionization energies for the atoms in the molecule implies that the correlation energy is taken care of. It is known that, in general, EHT performs rather poorly at predicting energy differences between isomers or even correct molecular geometries,[3] but there are some exceptions.[4] Charge differences, particularly between atoms of very different electronegativity, can be grossly exaggerated. The strength of EHT is that it gives a good qualitative picture

of the molecular orbitals (MOs). In fact it was looking at the MOs that came from EHT that Woodward and Hoffman devised their rules and won the Nobel Prize. It is now known that for the occupied MOs the corresponding eigenvalues agree reasonably well with experimentally determined ionization energies from photoelectron spectroscopy. They are typically 2 to 3 eV too low in energy. In 1988 a study found that EHT is also useful to determine unoccupied levels.[5] It is concluded that EHT can be used to study both occupied and unoccupied orbitals of a molecule, since it is directly useful for the calculation of excitation energies.[5]

The reasons for the good performance of EHT have elicited some very interesting theoretical analyses. The first one was published shortly after EHT was born. Lipscomb et al. suggested that EHT may be regarded as a method of simulating Hartree-Fock (HF) calculations by guessing the elements of the HF Hamiltonian matrix through the use of the Wolfsberg-Helmholz approximation.[6]

More recently, in a series of papers, Koch et al. have analyzed Rüdenberg's integral approximations[7] and their unrestricted and combined use in Molecular Orbital Theories of the Hartree-Fock type.[8, 9] They showed that, within the Hartree-Fock-Rüdenberg picture (HFR), EHT is compatible with the nonempirical Hartree-Fock method in Roothaan's form.[10] HFR thus explains why EHT turned out to be qualitatively successful.

With the abovementioned considerations, EHT is still undoubtedly a useful tool in areas where SCF calculations will not be feasible for some time to come. We must keep in mind that, as the EHT formalism does not take into account explicitly the electron–electron interaction, we should expect that the molecular orbital energies will be shifted downwards. Also a decrease in the energy difference between any pair of MOs is to be expected.

Both problems are minimized in molecular systems composed of hundreds or thousands of atoms in which a large or very large number of electrons are delocalized. Such systems have an extremely large number of molecular orbitals. The result, as the number of levels tends to infinity, is that MOs become very similar in energy over a certain range, forming an almost continuous band. In this case, and if we define zero energy (also called the Fermi Level or FL) as the midpoint between the Highest Occupied MO (HOMO) and the Lowest Unoccupied MO (LUMO) energies, the eigenvalues about zero will be almost the same in EHT, HF or DFT calculations. In the case of systems having a great number of π electrons, Extended Hückel Theory (EHT) can help to rationalize experimental results[11, 12] of SERS studies and even propose new interpretations of them (see below).

For all the above reasons we have selected the Extended Hückel Theory for calculating the electronic wavefunction. In all the EHT calculations the molecular geometry was optimized with Molecular Mechanics; this because of the system's size and also because we are dealing with normal bond lengths, bond angles and dihedral angles.

2.2. Minimal Molecular Models

The definition of a minimal molecular model was tackled by Contreras et al. a long time ago when studying lithium intercalation in 1T-TiS_2.[13–15] As they were studying a solid, their problem was to determine a minimal molecular model able to correctly describe the local interactions while retaining the main features of the electronic structure of the solid arising from its periodical properties. As a physical criterion they selected the invariance of the electronic chemical potential (ECP or μ) upon addition of basic units used to build the solid. Their results compared well with the available experimental data.

The ECP is related to the work function, a measurable physical property.[16] In Density Functional Theory, μ corresponds to the Fermi Level (or FL) at the limit $T \to 0$. Within the framework of Density Functional Theory, μ is defined as:[17]

$$\mu = \left[\frac{\partial E}{\partial N}\right]_v \cong \frac{I + A}{2} \tag{1}$$

where E is the electronic energy; N the number of electrons; v the external potential; I the ionization potential; and A the electron affinity. Working definitions for A and I are possible in Molecular Orbital theory.[18] Using Koopman's theorem we may use the approximations:[19]

$$I = -E_{\mathrm{HOMO}} \tag{2}$$

$$A = -E_{\mathrm{LUMO}} \tag{3}$$

where E_{HOMO} and E_{LUMO} are, respectively, the orbital energies of the HOMO and the LUMO. Therefore, μ can be evaluated as:

$$\mu \cong \frac{E_{\mathrm{HOMO}} + E_{\mathrm{LUMO}}}{2} \tag{4}$$

It is natural to ask if this approach is valid for all the single molecular structures that can be built starting from a basic unit. Below we present the results of the application of the above ideas to some surfaces of carbon, and some types of nanotubes (NT or NTs). We show that, for some cases, the use of the rule of the ECP invariance could be incorrect if it is not complemented with the analysis of other properties.

3. RESULTS AND DISCUSSION

3.1. Previous Results

A fundamental test for the use of the EHT method is its capacity to reproduce the band structure of molecular systems for which a great number of experimental and theoretical results are known. We were specifically interested in the first valence and first conduction bands (BV

and CB respectively), whose structure and gap define insulators, semiconductors and metals. An associated concept is that of density of states (DOS), which describes the energy levels per unit energy increment. The general procedure to obtain the band structure of a single molecule within any standard quantum chemical scheme (semiempirical, *ab initio* or density functional) is the following. A quantum chemical calculation is carried out to obtain the complete eigenvalue spectrum. The band structure is then built by synthesizing the whole eigenvalue spectrum into a DOS spectrum by convolution using a mathematical function with a certain width.

Our first step consisted in determining the best values for the half-width and the scanning distance (the energy distance between each calculated DOS value) of the mathematical function used to obtain the theoretical DOS spectrum. We examined a Gaussian function, a Lorentzian function and a mixture of both.[20] For this task, a microscopic model of buckminsterfullerene C_{60} consisting of seven molecular orbitals (3 occupied and 4 empty) was considered. We excluded other MOs because they are energetically well separated from the selected ones and therefore they should have no influence on the convoluting process. The MOs result from a Density Functional Theory calculation (full geometry optimization) with the Amsterdam Density Functional (ADF) package of programs.[21–23] The local density approximation characterized by the homogeneous electron gas exchange,[24] together with the VWN parameterization[25] was used. The gradient-corrected Becke[26] and Perdew[27] functionals for exchange and correlation are included, respectively. A STO basis set of double-ζ + polarization quality was used to describe the valence electrons of all atoms. The 1s electrons were treated as frozen core shells. This high level calculation was necessary to compare later these results with EHT ones.

The results showed that a purely Gaussian function of the form:

$$\mathrm{DOS}(E) = \frac{1}{(2\pi)^{1/2}\sigma} \exp 2 \sum_i \left(-\frac{(E - E_i)^2}{2\sigma^2} \right) \qquad (5)$$

with values for both, σ and the scanning distance, of 0.1 eV.[20] The DOS spectrum for C_{60} obtained with this function (see Fig. 1) reproduces experimental results obtained with photoemission and inverse photoemission techniques very well. Therefore, this function has been used later in all our work. We must stress that C_{60} is a medium-sized molecule; therefore we should not expect the number of π MOs to be great enough to become separated by small energy intervals.

The reliability of the EHT methodology to calculate the total DOS distribution curve was tested with two medium-sized X_{60} (X = C, N) molecular systems.[28] We used EHT, Density Functional (B3LYP/6-311G**) and *ab initio* Hartree-Fock (RHF 6-31G** basis set) methods. The results showed that EHT is only reliable in the cases

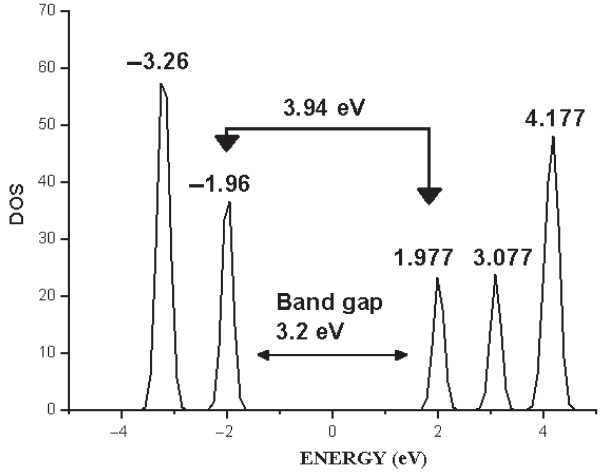

Fig. 1. Simulation of the experimental DOS spectrum for C_{60}. The Fermi level is at $E = 0.0$ eV (from Ref. [20]).

of the first valence and conduction bands of these systems. For the rest of the Density of States distribution curve EHT performs badly. The sources of error of EHT come from the non-inclusion of the electron–electron interaction (for both systems) and from incorrect results regarding the relative ordering of the MO degeneracies in the case of N_{60} (this last system has no π electrons). Therefore a general tentative conclusion is that EHT will not perform well for medium-sized molecules and/or for molecules having no π electrons.

At the same time we were analyzing bigger zigzag and armchair nanotubes searching for the existence or not of a minimal molecular model.[29] This kind of nanotubes, and also graphene layers, has a very special electronic structure. At the extremities of nanotubes, and also at the border of graphene layers and at the surface of diamonds we find carbon atoms with a free valence (also called dangling bonds or free valences). Our experience indicates that the MOs formed with these free valences are located around the Fermi Level in between the π MOs. Therefore, all calculations carried out by filling these free valences with hydrogen atoms are incorrect. This is so because hydrogenation of the free valences produces σ MOs located very far from the Fermi Level, therefore altering significantly the electronic structure of the system.

Since for any NT with constant diameter there is an infinite number of structures differing only in their length, the central question is this: is there a minimal length (ML) for a given nanotube where one can reasonably assert that the main features of its electronic and band structures calculated at that point can be extrapolated to longer ones? To answer this question, the following kinds of nanotubes were selected for the study: an armchair (5, 5) set of NTs with metallic properties, a set of metallic (9, 0) zigzag NTs, and a set of semiconducting (10, 0) zigzag NTs. The procedure to construct the elements of each set was the following. The first member of the family is a NT composed

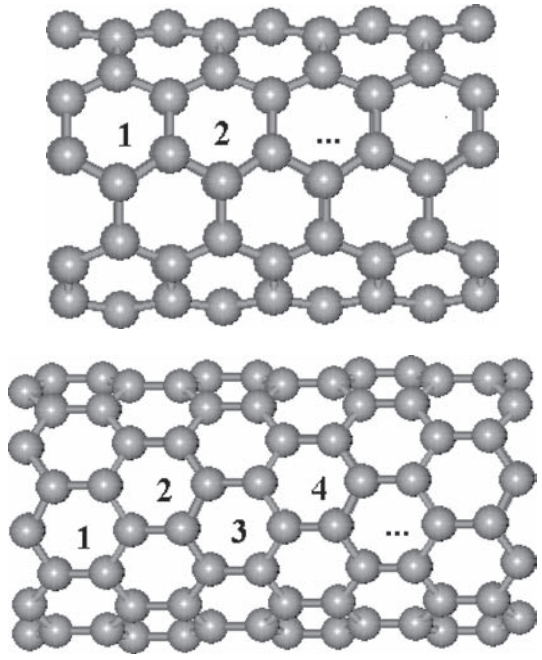

Fig. 2. Numbering of units for armchair and zigzag nanotubes (from Ref. [29]).

by only one rod (called unit) of benzene rings rolled in the appropriate way. The second member is a NT composed by two fused rods of benzene rings, and so on (see Fig. 2).

The Extended Hückel Theory results for these three kinds of nanotubes are shown in Figures 3 to 5. Our main result can be generalized as a conjecture stating that all pure carbon armchair and zigzag NTs have a minimal length defining the boundary between large molecules (or short NTs) and nanotubes properly speaking.[29] The corollary is that any NT with a length falling below the ML should be treated only as a big molecule and not as a nanotube whose electronic properties are similar to the ones of longer NTs. Notice also that the ECP curves are very different for pure and hydrogenated NTs.

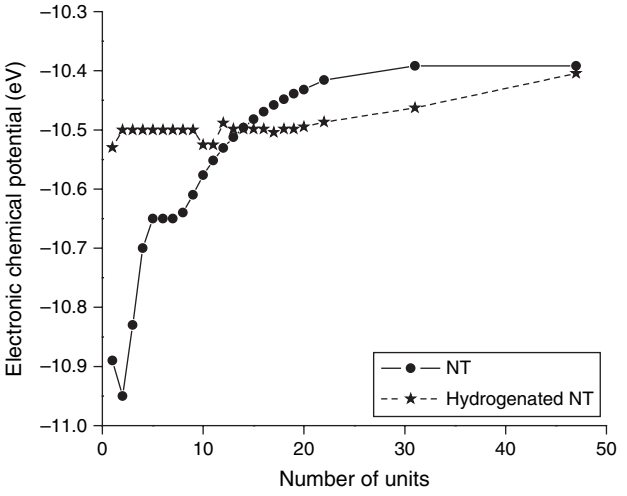

Fig. 4. ECP curve for the family of metallic $(9, 0)$ zigzag nanotubes (from Ref. [29]).

To test the goodness of EHT we studied the following problem. There are two basic types of metal nanotubes: armchair and zigzag (there are also chiral NTs). The difference is the direction in which the graphite sheet is rolled. The sheet's rows of carbon atoms hexagons run along the nanotube axis in armchair nanotubes and around its circumference in zigzag nanotubes. All armchair nanotubes are metallic, as are one-third of all possible zigzag nanotubes, but recent experimental evidence has challenged this view.

Lieber et al. used low-temperature scanning tunneling microscopy to characterize the atomic structure and local density of states of metallic zigzag and armchair single-walled carbon nanotubes (SWNTs).[30] Their data, recorded for $(9, 0)$, $(12, 0)$ and $(15, 0)$ zigzag SWNTs, show the

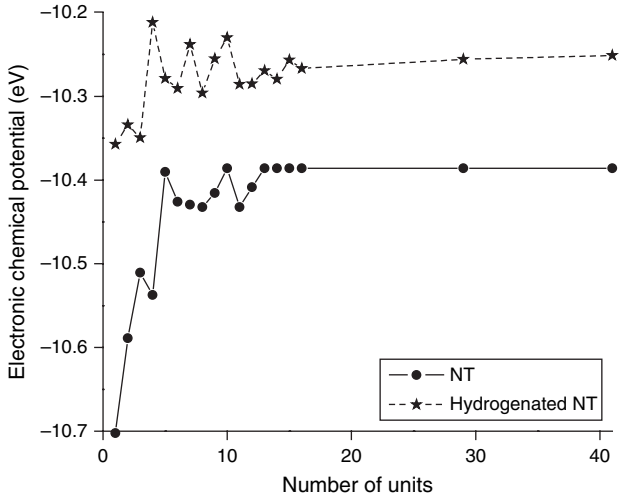

Fig. 3. ECP curve for the family of metallic $(5, 5)$ armchair nanotubes (from Ref. [29]).

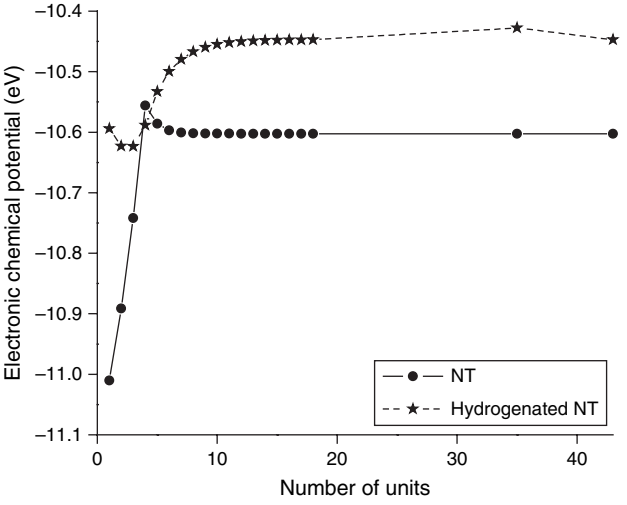

Fig. 5. ECP curve for the family of semiconducting $(10, 0)$ zigzag nanotubes (from Ref. [29]).

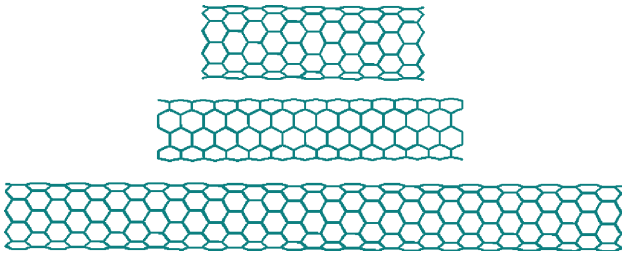

Fig. 6. From top to bottom: A (10, 0) zigzag NT composed of 11 units, a (5, 5) armchair NT composed of 13 units, and a (9, 0) zigzag NT composed of 31 units (from Ref. [31]).

existence of gap-like structures at the Fermi energy. Consequently, they suggested that these metallic zigzag NTs are in fact small-gap semiconductors. Their results also show that isolated armchair SWNTs have neither gaps nor pseudo gaps. No clear and simple explanations have been offered to account for these results. To see if EHT results can provide an explanation for those results, we made use of the concept of minimal length to study the (5, 5) metallic armchair, (9, 0) metallic zigzag and (10, 0) semiconducting zigzag NTs[29] (see Fig. 6). For each of them we performed an EHT calculation to obtain the eigenvalues.[31] As the electronic conductance in a NT depends only on its π electrons, the Density of States curve must include only those eigenvalues associated with a π MO (the π eigenvalue spectrum). For this purpose a grand total of 1,606 MOs belonging to the three NTs were individually plotted and visually inspected to classify them as π, σ or dangling. Very few cases of mixing were observed, all of them being energetically very far from the Fermi level. For each nanotube the corresponding π DOS curves were calculated through a convolution of the π eigenvalue spectrum with Eq. (5). Figure 7 shows the π DOS curve for the (10, 0) zigzag nanotube. As expected for a semiconducting system, we observe a gap of about 0.3–0.4 eV between the valence (at the left side of the Fermi Level)

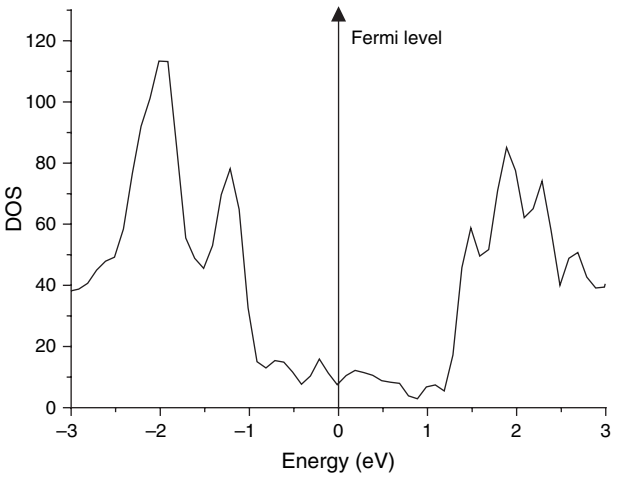

Fig. 8. π Dos curve for the metallic (5, 5) NT.

and conduction (at the right side of FL) bands. Knowing that EHT underestimates the energy gap, this result compares well with more sophisticated studies.[32] Figure 8 shows the π DOS curve for the (5, 5) armchair NT. We can see that there are no impediments for the electrons to flow from the valence band (left side of the FL) to at least all the available states in the conduction band between the Fermi Level and a small pseudo gap located at about 0.9 eV. This is congruent with fully metallic behavior. Figure 9 shows the π DOS curve for the (9, 0) zigzag NT. No gap is seen between the valence and conduction bands. Here, and contrarily to the case of the (5, 5) NT, the full conduction band is accessible. Nonetheless, only the electrons occupying the states between the Fermi Level and a pseudo gap located at -0.6 eV may flow freely towards the conduction band. This smaller number of electrons is the reason for the less metallic behavior of the zigzag SWNTs. We conclude therefore that zigzag SWNTs are not small-gap semiconductors but semimetallic molecular systems.[31]

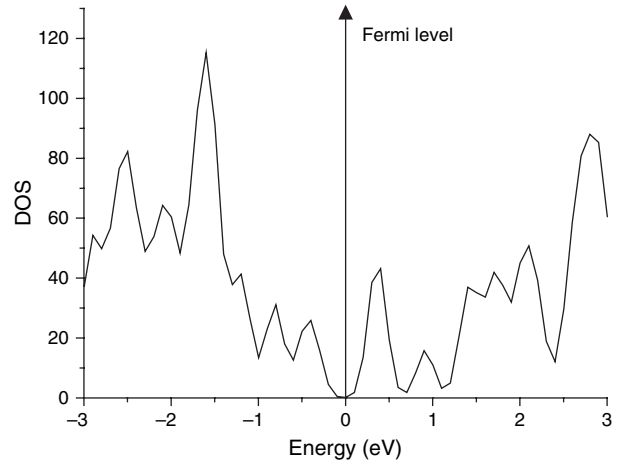

Fig. 7. π DOS curve for the semiconducting (10, 0) NT.

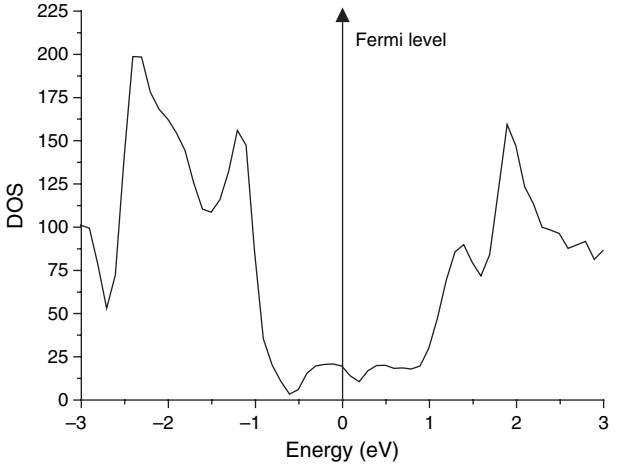

Fig. 9. π DOS curve for the metallic (9, 0) NT.

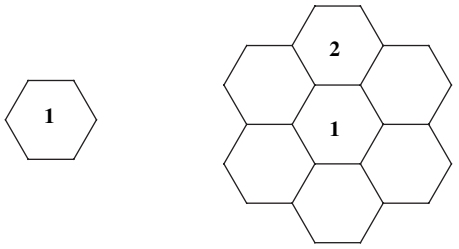

Fig. 10. The left side shows the basic unit of B, C and N surfaces. The right side shows the next unit.

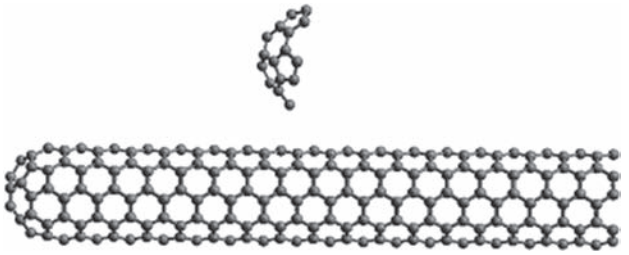

Fig. 11. Half-capped NT. The upper part shows the basic unit. The lower part shows the same basic unit plus 340 atoms.

3.2. New Results

All these results prompted us to study the existence or not of minimal molecular models for new and different molecular systems. Below we present new results for surfaces of carbon and for capped and half-capped NTs. The surfaces were built by considering a basic unit of six atoms (see Fig. 10). Each member of the series was obtained by surrounding the previous one with six-membered rings. We also studied the series generated by filling the free valences with hydrogen atoms, this because we were interested in the study of the variation of the HOMO and LUMO energies (E_{HOMO} and E_{LUMO}) when the structure grows. The first group of nanotubes is one derived from the C_{60} fullerene in which one end is closed (half-capped NT, see Fig. 11). In this case, the open part of the NTs is of the armchair type. The next member of this series is generated by adding a circular row of ten carbon atoms, etc. The second group of NTs consists of the hydrogenated members of the first group (Fig. 12). In the next two NT groups both ends are closed (Fig. 13). The first one (called "Capped-A") is generated from the C_{70} fullerene (with D_{5h} symmetry) by intercalating consecutively rods of ten carbon atoms. The second one ("Capped-B") is generated from the C_{60} fullerene (with I_h symmetry that is lost in the next members of this series).

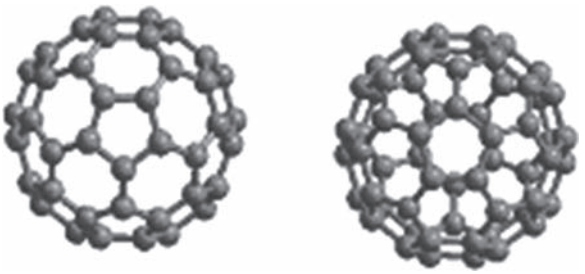

Fig. 13. The left side shows a view along the maximal symmetry axis of group A of capped NTs. The right side shows the same view for group B of capped NTs.

Figure 14 shows the variation of ECP, E_{HOMO} and E_{LUMO} in growing planar sp^2 carbon surfaces (or graphenes). It can be seen that the values of E_{HOMO} and E_{LUMO}, that were well separated from the first to the seventh members, suddenly become equal at the level of the ninth structure. How can we interpret this result? As we said before, we expect that EHT results begin to approach higher-level results only when the MO energies come close enough to form bands. In the case of the ninth structure, the first seventy occupied MOs span a range of only 1 eV. The same happens for the fist 36 empty MOs. Therefore, at the level on the ninth structure, we are not observing the formation of a triplet state but the transition from semiconducting structures to metallic ones. Experimental results on highly ordered pyrolitic graphite show that it behaves as a semimetal.[34] Let us remember that a semimetal is a material with a small overlap in the energy of the conduction and valence bands. We should expect that EHT results show that the bottom of the conduction band (i.e., the HOMO) of the ninth structure is situated in a different place of the ninth structure than the top of the valence band (i.e., the LUMO) but with some overlap between them. Figures 15 and 16 show, respectively, the electron density distribution for the HOMO and LUMO of this structure. Comparison of both figures shows that the HOMO and LUMO electronic densities are localized on the same atoms only in a few cases. This indicates that there is a physical (spatial) limitation for the electron flow from the valence band to the conduction band. Therefore, EHT results again succeed in explaining experimental results. Therefore the ninth structure, composed of 489 carbon

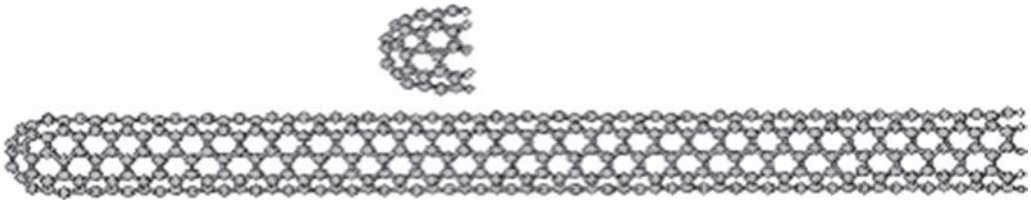

Fig. 12. Half-capped hydrogenated NT. The upper part shows the basic unit. The lower part shows a member of this series.

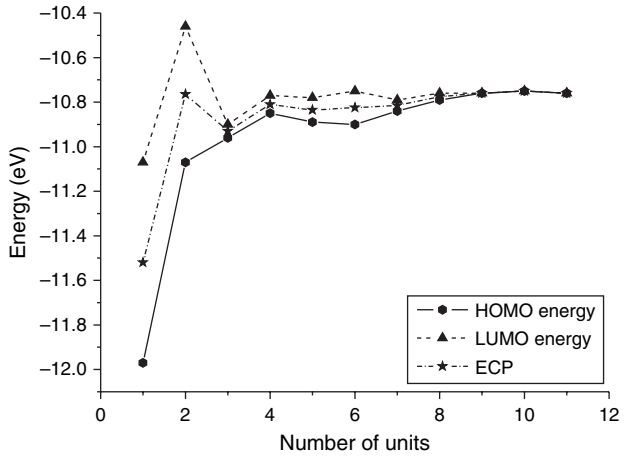

Fig. 14. Variation of ECP, E_{HOMO} and E_{LUMO} in carbon surfaces.

atoms, seems to be a good candidate to study the main electronic properties of a graphite monolayer.

An important conclusion is that the curve representing the variation of the ECP is not enough to get a good definition of a minimal molecular model. It seems necessary to carry out an analysis of the variation of E_{HOMO} and E_{LUMO} and, when needed, a study of the electronic densities of the HOMO and LUMO.

Figure 17 shows the variation of ECP, E_{HOMO} and E_{LUMO} in growing sp^2 planar carbon graphene surfaces in which the free valences have been filled with hydrogen atoms. We may see that the saturation of the free valences produces a constant ECP value almost from the beginning of the series. E_{HOMO} and E_{LUMO} converge harmoniously until the eleventh structure, when their values become equal. This shows again a transition between semiconducting and semimetallic behaviors (electron density maps of the HOMO and LUMO are not shown here but they are similar

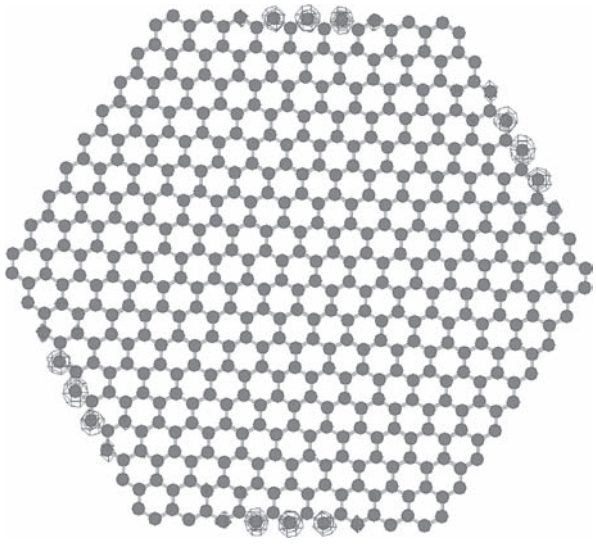

Fig. 15. Distribution of the electron density of the HOMO in the ninth structure (Isodensity = 0.0005 e).

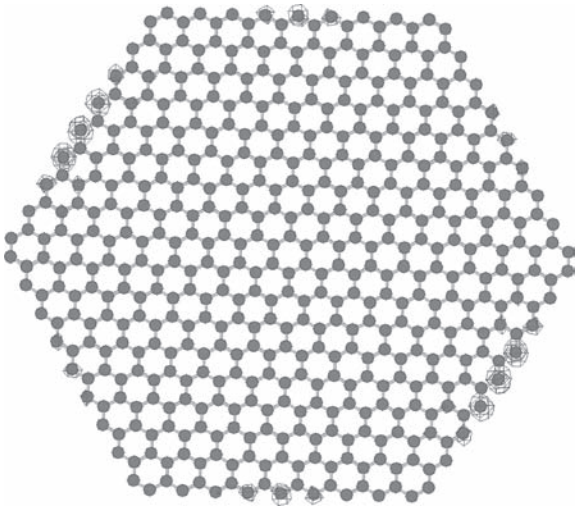

Fig. 16. Distribution of the electron density of the LUMO in the ninth structure (Isodensity = 0.0005 e).

to the case of graphene surfaces). There is no experimental information on these structures.

Figure 18 shows the variation of ECP, E_{HOMO} and E_{LUMO} in half-capped nanotubes. A surprising finding is that there appear to be regions in which HOMO and LUMO are degenerate and regions in which they are not. An analysis of the electronic structures of HOMO and LUMO in all the members of this series indicates that both are dangling MOs. For the moment we cannot offer an explanation of this fact, but we may discard a metallic behavior in these structures because the energy of the first occupied π MO is well separated from the energy of the first empty π MO. As no experimental information exists on these molecular systems we shall suggest, only as a hypothesis, that the fundamental state of some of the members of this series is a triplet because HOMO and LUMO are located on the same atoms. If this is true, some of these systems are

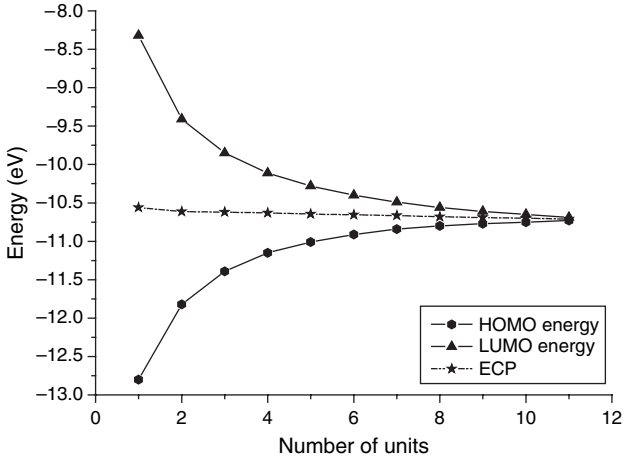

Fig. 17. Variation of ECP, E_{HOMO} and E_{LUMO} in carbon surfaces saturated with H atoms.

RESEARCH ARTICLE

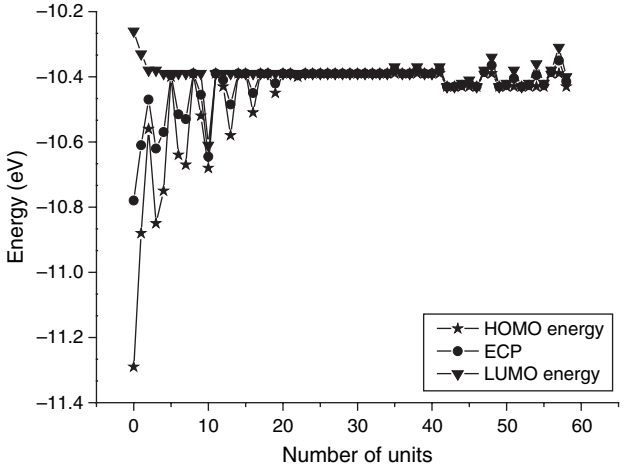

Fig. 18. Variation of ECP, E_{HOMO} and E_{LUMO} in half-capped nanotubes.

not chemically stable under normal atmospheric conditions (they will react with ozone, some nitrogen oxides, etc.). This prediction will be a good test for whenever the first experimental results on these systems appear.

Figure 19 shows the variation of ECP, E_{HOMO} and E_{LUMO} in the family of hydrogenated half-capped nanotubes. The ECP tends to stabilize slowly. The behavior of E_{HOMO} and E_{LUMO} is oscillating but convergent. The value of the band-gap decreases with increasing NT length; however, this decrease is not monotonic but shows a well-defined oscillation. This oscillation has also been reported for EHT and DFT studies of a set of (6, 6) nanotubes.[34] This phenomenon was explained in terms of periodic changes in the bonding characteristics of the HOMO and the LUMO. In EHT studies of 2-D polyphenanthrenes band-gap oscillations also appear.[35] These facts rule out this oscillation as an artifact of the calculation method. As the HOMO and the LUMO are of π nature these systems behave as semiconductors. It is important to notice the great differences in the results between pure carbon half-capped NTs and hydrogenated ones: it is an unmistakable example of why hydrogenated nanotubes cannot be used to model pure carbon ones.

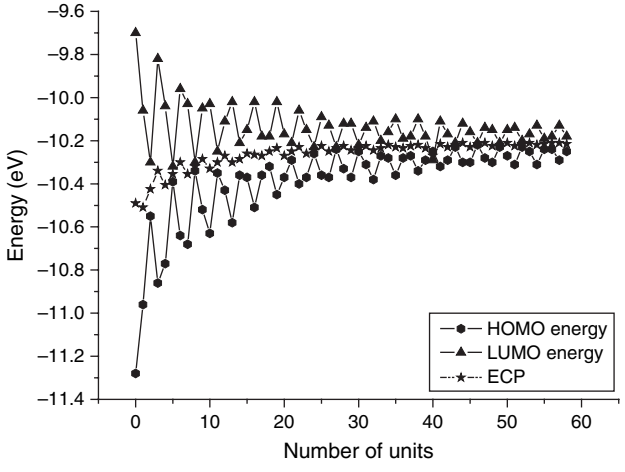

Fig. 19. Variation of ECP, E_{HOMO} and E_{LUMO} in half-capped hydrogenated nanotubes.

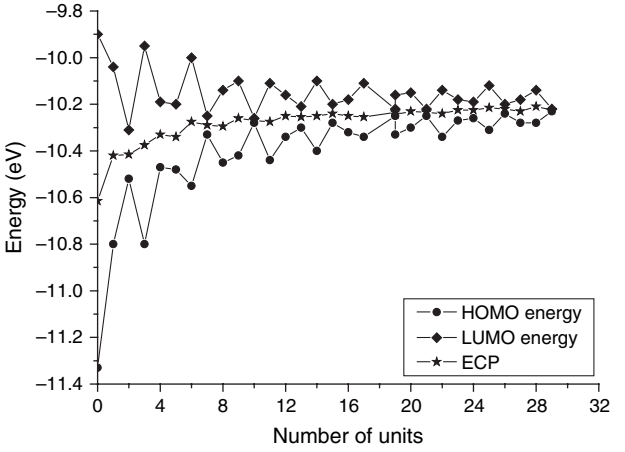

Fig. 20. Variation of ECP, E_{HOMO} and E_{LUMO} in group A of capped nanotubes.

Figure 20 shows the variation of μ, E_{HOMO} and E_{LUMO} in group A of capped nanotubes. HOMO and LUMO are of π nature. In the last member studied the E_{HOMO} and E_{LUMO} difference is of about 0.01 eV, suggesting the appearance of metallic behavior at least in some members of this series. More studies on longer capped NTs are needed to see is the band-gap oscillation disappears or not.

Figure 21 shows the variation of μ, E_{HOMO} and E_{LUMO} in group B of capped nanotubes. Like group A, HOMO and LUMO are of π nature. In some structures the E_{HOMO} and E_{LUMO} difference is of about 0.01 eV. Interestingly, the oscillatory behavior of the band-gap is different here. There are two structures with well separated E_{HOMO} and E_{LUMO} values, followed by one in which E_{HOMO} and E_{LUMO} values tend to be almost equal. Up to now, we have no clear explanation for these differences.

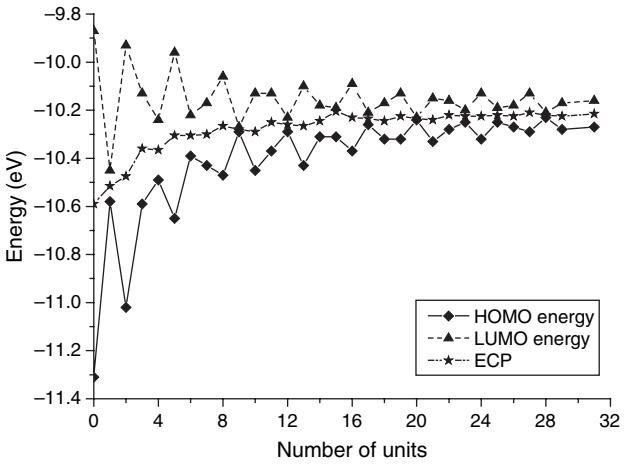

Fig. 21. Variation of ECP, E_{HOMO} and E_{LUMO} in group B of capped nanotubes.

4. CONCLUSIONS

It is now clear that the analysis of only the ECP invariance does not guarantee the definition of a minimal molecular model. We must add the study of the E_{HOMO} and E_{LUMO} values and the nature and location of all the respective MOs. For example, lacking some of these results a metallic behavior may be confused with a triplet state.

All the results presented above indicate that Extended Hückel Theory is still a valuable tool for the study of the electronic structure of molecular systems possessing great numbers of π electrons. When computing capacity increases in such a way that we could easily deal with all the above systems, EHT will be useful for even larger molecular structures.

References

1. R. Hoffmann, *J. Chem. Phys.* 39, 1397 (**1963**).
2. M. Wolfsberg and L. Helmholz, *J. Chem. Phys.* 20, 837 (**1952**).
3. D. C. Young, Computational Chemistry, Wiley-Interscience, New York (**2001**).
4. M. S. Jhon, U.-L. Cho, L. B. Kier, and H. Eyring, *Proc. Nat. Acad. Sci. USA* 69, 121 (**1972**).
5. E. Lindholm and J. Li, *J. Phys. Chem.* 92, 1731 (**1988**).
6. F. P. Boer, M. D. Newton, and W. N. Lipscomb, *Proc. Natl. Acad. Sci. USA* 52, 890 (**1964**).
7. K. Rüdenberg, *J. Chem. Phys.* 19, 1433 (**1951**).
8. W. Koch, *Int. J. Quant. Chem.* 76, 148 (**2000**).
9. W. Koch, B. Frey, J. F. Sánches, and T. Scior, *Z. Naturforsch.* 58A, 756 (**2003**).
10. C. C. J. Roothaan, *Rev. Mod. Phys.* 23, 69 (**1951**).
11. P. Leyton, J. S. Gómez-Jeria, S. Sanchez-Cortes, C. Domingo, and M. Campos-Vallette, *J. Phys. Chem. B* 110, 6470 (**2006**).
12. P. Leyton, I. Córdova, P. A. Lizama-Vergara, J. S. Gómez-Jeria, A. E. Aliaga, M. M. Campos-Vallette, E. Clavijo, J. V. García-Ramos, and S. Sanchez-Cortes, *Vibr. Spectrosc.* 46, 77 (**2008**).
13. F. Mendizábal, R. Contreras, and A. Aizman, *Int. J. Quant. Chem.* 56, 819 (**1995**).
14. F. Mendizábal, R. Contreras, and A. Aizman, *J. Mol. Struct. (Theochem)* 335, 161 (**1995**).
15. F. Mendizábal, R. Contreras, and A. Aizman, *J. Phys.: Condens. Matter* 9, 3011 (**1997**).
16. N. W. Ashcroft and N. D. Mermin, Solid State Physics, Holt, Rinehart and Winston, New York (**1978**).
17. R. G. Parr, R. A. Donnelly, M. Levy, and W. E. Palke, *J. Chem. Phys.* 68, 3801 (**1978**).
18. R. G. Pearson, *Acc. Chem. Res.* 26, 250 (**1993**).
19. T. A. Koopman, *Physica* 1, 104 (**1933**).
20. J. S. Gómez-Jeria, *J. Chil. Chem. Soc.* 51, 905 (**2006**).
21. G. te Velde, F. M. Bickelhaupt, S. J. A. van Gisbergen, C. F. Guerra, E. J. Baerends, J. G. Snijders, and T. Ziegler, *J. Comput. Chem.* 22, 931 (**2001**).
22. C. F. Guerra, J. G. Snijders, G. te Velde, and E. J. Baerends, *Theor. Chem. Acc.* 99, 391 (**1998**).
23. ADF-2004.01, SCM, Theoretical Chemistry, Vrije Universiteit, Amsterdam, The Netherlands.
24. J. C. Slater, Quantum Theory of Molecules and Solids, McGraw-Hill, New York (**1974**), Vol. 4.
25. H. Vosko, L. Wilk, and M. Nusair, *Can. J. Phys.* 58, 1200 (**1980**).
26. A. D. Becke, *Phys. Rev. A* 38, 3098 (**1988**).
27. J. P. Perdew, *Phys. Rev. B* 33, 8822 (**1986**).
28. J. S. Gómez-Jeria, *J. Chil. Chem. Soc.* 51, 1061 (**2006**).
29. J. S. Gómez-Jeria and F. Soto-Morales, *J. Chil. Chem. Soc.* 50, 635 (**2005**).
30. M. Ouyang, J.-L. Huang, C. L. Cheung, and C. M. Lieber, *Science* 292, 702 (**2001**).
31. J. S. Gómez-Jeria, *J. Chil. Chem. Soc.* 52, 1198 (**2007**).
32. J. O'Keeffe, C. Wei, and K. Cho, *Appl. Phys. Lett.* 80, 676 (**2002**).
33. J.-P. Issi, Graphite and Precursors, edited by P. Delhaès, Gordon and Breach Science Publishers, Amsterdam (**2001**), pp. 45–70.
34. A. Rochefort, D. R. Salahub, and P. Avouris, *J. Phys. Chem. B* 103, 641 (**1999**).
35. K. Yoshizawa, K. Yahara, K. Tanaka, and T. Yamabe, *J. Phys. Chem. B* 102, 498 (**1998**).

Received: 2 July 2008. Accepted: 10 July 2008.